Chinese Chemical Letters 33 (2022) 1599–1603

Contents lists available at ScienceDirect

Chinese Chemical Letters

journal homepage: www.elsevier.com/locate/cclet

The marriage of sealant agent between structure transformable silk fibroin and traditional Chinese medicine for faster skin repair

Rongjun Zhang[a,b,1], Youbin Zheng[c,1], Tianqing Liu[d,1], Ning Tang[d,1], Lianzhi Mao[e], Lihan Lin[a], Jiahui Ye[a], Luoyijun Xie[a], Wenwen Hu[d], Weiwei Wu[d,*], Wenzhen Liao[e,*], Miaomiao Yuan[a,*]

[a] The Eighth Affiliated Hospital, Sun Yat-sen University, Shenzhen 518033, China
[b] Institute of Molecular Medicine (IMM), Renji Hospital, Shanghai Jiao Tong University School of Medicine, Shanghai 200240, China
[c] Department of Chemical Engineering and Russell Berrie Nanotechnology Institute, Technion-Isr1ael Institute of Technology, Haifa 3200003, Israel
[d] School of Advanced Materials and Nanotechnology, Interdisciplinary Research Center of Smart Sensors, Xidian University, Xi'an 710126, China
[e] Department of Nutrition and Food Hygiene, School of Public Health, Southern Medical University, Guangzhou 510515, China

ARTICLE INFO

Article history:
Received 5 June 2021
Revised 1 September 2021
Accepted 3 September 2021
Available online 10 September 2021

Keywords:
Rehmanniae radix preparata
Silk fibroin
Sealant agent
Photo-thermal effect
Skin repair

ABSTRACT

Fast skin repair is critical for less infection, less pain and high quality of life, which is still limited with undesirable rehabilitation speed and side effects. Currently, laser-activated silk sealant agent without suture and gauze has been demonstrated promising for fast skin repair taking advantage of its structural transformation after heating. Nevertheless, more efficient healing effects and less side effects of laser-activated silk sealant agent remains challenging due to absence of suitable photo-thermal materials and robust/biomimetic protein materials. In this work, the marriage between silk protein and *Rehmanniae radix preparata* (a kind of the traditional Chinese herb) has been demonstrated as a novel and effective way to achieve an excellent healing effect for skin repair. The non-toxicity, high photothermal conversion efficiency and healing mechanism are systematically studied and proved. This new methodology might shed a new light for combining dark traditional Chinese medicine and silk fibroin for advanced wound healing technology.

Skin, as the largest and most vulnerable organ of human body, protects various tissues and organs from physical/chemical injuring and pathogenic microorganisms infection [1-3]. The injury and healing of skin frequently and inevitably happen in our daily life. Therefore, the fast healing of skin is critical for less infection, less pain and higher quality of life [4]. Regarding of this issue, iodophor and gauze are frequently employed in the process of incision and wound suture in the surgical skin repair, which are limited with skin and soft-tissue infection [5]. In addition, many suture glues are used conveniently along with undesirable healing effects, which could be useless or even harmful ascribing to the ineffective angiogenesis [6]. Therefore, besides considering the feasibility for clinical trials, effective, convenient and well-tailored healing process is also important on the wound healing [7]. Highly biocompatible and natural biomaterials are good candidate for skin repair therapy to overcome aforementioned hinderances [8-10].

Silk fibroin [11], a natural protein extracted from silk cocoons, has become one of the most promising silk-based materials in skin engineering subject in recent years due to its non-toxicity, enhanced cell migration ability (β-sheet), degradable property and reproducible source [12]. In addition, its structural transformation form α-helix (as-prepared) to β-sheet (heated) or even tertiary structure [13] over 60 °C contribute to construct robust micro skeleton, newborn of blood capillary and migrate of fibroblasts or keratinocytes [14], which are useful for fastening the skin healing process [15,16]. Otherwise, silk fibroin has been verified with low immune reaction [17] and inflammatory response when interacts with skin wound closely [18]. Therefore, silk fibroin has been considered to be a promising biomaterial in skin repair [19,20].

The structural transformation of silk fibroin requires a thermal source to ensure the temperature over 60 °C. Recent studies have showed that laser-activated skin repair is a promising approach for skin repair without iodophor, suture and gauze [21]. Near Infrared (NIR) [22], mainly ranging from 780 nm to 1100 nm [23], could

* Corresponding authors.
E-mail addresses: wwwu@xidian.edu.cn (W. Wu), wenzhenliao@163.com (W. Liao), yuanmm2019@163.com (M. Yuan).
[1] These authors contribute equally to this work.

https://doi.org/10.1016/j.cclet.2021.09.018
1001-8417/

elevate local temperature by absorbing and converting NIR laser to heat [24-26]. NIR laser have been introduced into clinical application owing to unresponsive and inactive to skin. For example, the laser-activated nanosealants (LANS) combining gold nanorods with silk fibroin have been used in skin incisions in mice, and the results revealed that LANS could increase the mechanical strength and repair the incision faster [27]. Gold nanorod is kind of precious metal materials which could not been widely used. Therefore, it is still challenging to develop a nontoxic, cheap and highly efficient laser-activated silk sealant agent for the future clinical applications.

Rehmanniae radix preparata (RRP) [28], a common drug of traditional Chinese medicine with dark color [29] generated from *Rehmannia glutinosa Libosch*, has a good ability to absorb NIR laser and then convert the photon to heat by photo-thermal effect [30]. In addition, previous pharmacological researches had demonstrated that RRP, containing various compounds such as polysaccharides, oligosaccharides, glycosides andiridoid glycosides [31], possesses wide actions of boosting essence, filling bone marrow, enhancing immune activation and supplementing blood, which were superb for skin healing [32]. Moreover, many researches also demonstrated that RRP could be used for inflammatory diseases [33]. But few studies of the photothermal ability of RRP, and whether the RRP could be an activated agent for silk sealant remain unclear. Sealant was kind of a protective agent in wound healing region which could protect wound from continuous bacterium infection and improve healing effect. Therefore, it is reasonable to assume that the marriage of sealant agent between structure transformable silk fibroin and RRP might a good cocktail therapy for faster skin repair.

In this study, we studied the photothermal conversion of RRP, and combined the natural material RRP and silk fibroin as a new sealant agent for skin repair. In addition, the healing mechanism were studied and proved. Prospectively, as developed RRP@silk film in this study might be a promising agent potential for faster skin repair.

In order to increase the release amount of β-sheet structure from the composite film, the thermal response properties of RRP were first investigated. RRP was a natural pharmaceutical preparation which originated from *Rehmannia glutinosa Libosch*. By grinding it with PBS buffer (pH 7.4), RRP solutions with different concentrations can be obtained (Fig. 1a). As shown in Fig. 1b, the vis-NIR absorption spectrum results exhibited that the absorption of RRP solutions decreased smoothly with the increasing wavelength ranged from 700 nm to 900 nm, which was similar as the performance of sodium humate [34] and Au NPs [35]. In order to keep consistence with the NIR laser used in later experiments, the absorption results of RRP solutions at 808 nm were also studied (Fig. 1c). These results presented that the absorption values were close to linear with the increase of concentrations and the fitting variance (R^2) was 0.97. These experiments proved that RRP solutions were unexceptionable dispersity and compatible.

To evaluate the photo-thermal performance of RRP solutions, an irradiation of 808 nm laser was used in following studies. As shown in Fig. 1d, the RRP solutions exhibited conspicuous temperature elevation with time increment compared to PBS buffer. Meanwhile, the degree of temperature elevation gradually enhanced with increment of RRP concentrations. As for the RRP solution with 100 mg/mL concentration, the temperature raised from 28.5 °C to 60.9 °C within 10 min. These results demonstrated that RRP solution could effectively convert NIR laser to heat, which was high enough for photothermal therapy [36].

To further assess photothermal ability, the RRP solution (100 mg/mL) was irradiated of 808 nm laser with a gradient output power (0.5, 0.75, 1 and 2 W/cm^2) for 10 min. Fig. 1e had showed that RRP solutions exhibited noteworthy temperature increment. As above, RRP solutions were presented wonderful photothermal conversion ability. In addition, we investigated the photothermal stability of RRP solutions. As shown in Fig. 1f, the temperature change of RRP solutions remained almost the same during the four-repeated irradiation cycles with 10 min laser on and 10 min laser off, suggesting an excellent photothermal stability of RRP solutions. Based on all above data, the photothermal conversion efficiency (η) of RRP solutions was calculated according to a previously reported method [37]. The η value of RRP solution was determined to be 63.7% (Fig. 1g), much higher than that many photothermal agents reported previous including donor-acceptor structured conjugated polymers [38], MoS_2-Au nanocomposites [39] and amphiphilic semiconducting oligomer DPP-BT-PEG [40]. The high photothermal conversion efficiency of RRP solutions may be attributed to strong intramolecular charge-transfer interactions [41], strong heat generation of unnumbered melanin [42] and few heat loss [43].

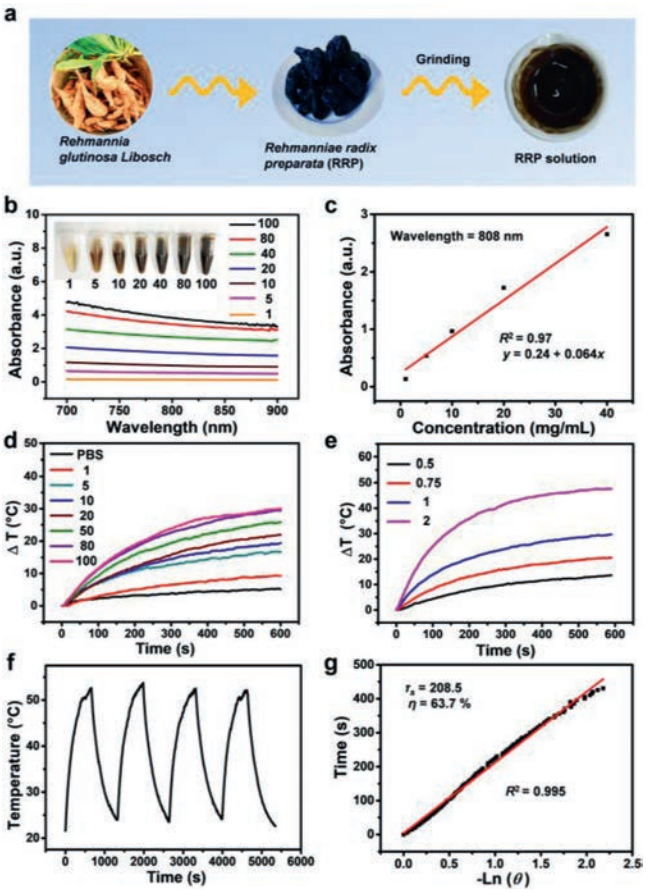

Fig. 1. Preparation and photothermal performance of RRP solution. (a) Schematic representation of the formation of RRP solution. (b) The vis-NIR absorption spectra of RRP solutions (mg/mL). (c) The fitting curve of the absorbance of RRP solutions at 808 nm as a function of concentrations, and the inset was digital photograph of different concentrations of RRP solutions. (d) Temperature elevation of RRP solutions (mg/mL) with different concentrations and PBS under an 808 nm laser irradiation (10 min, 1 W/cm^2). (e) Temperature elevation of a concentration of 100 mg/mL RRP solutions with different power densities (0.5, 0.75, 1, and 2 W/cm^2) under an 808 nm laser irradiation. (f) Heating/cooling curves of RRP solution with a concentration of 100 mg/mL for four times repeated irradiation cycles (1 W/cm^2). (g) The fitting linear curve of time data *versus* –Ln (θ) acquired from the cooling period, and the time constant (τ_s) for heat transfer was calculated to be 208.5 s.

According to the above data, we had a brief knowledge about the photothermal ability and stability of RRP solutions. In order to deeply evaluate the photothermal performance of silk and RRP film, the preparation process of RRP@silk film was illustrated in Fig. 2a [44]. To obtain the excellent photothermal performance of

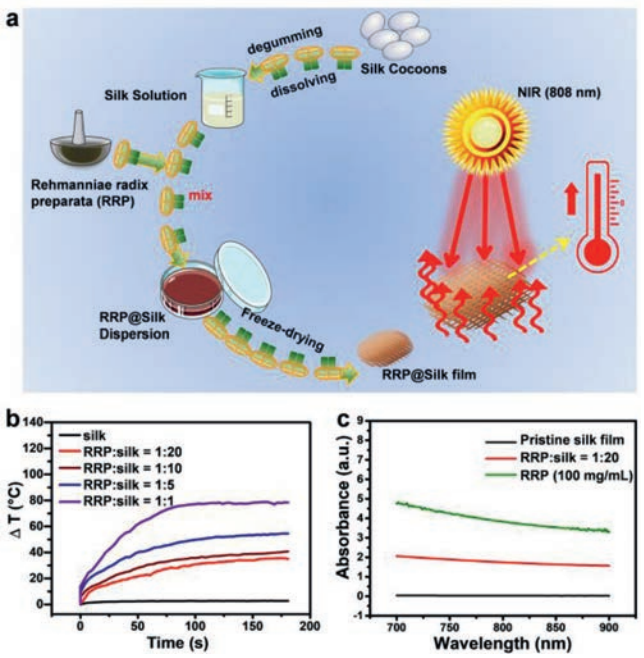

Fig. 2. Preparation of RRP@silk film. (a) Schematic representation of the formation of RRP@silk film. (b) Temperature elevation of RRP@silk film with different proportion of silk and RRP solution under an 808 nm laser irradiation (10 min, 1 W/cm^2). (c) The vis-NIR absorption spectra of RRP solutions, pristine silk film and RRP@silk film.

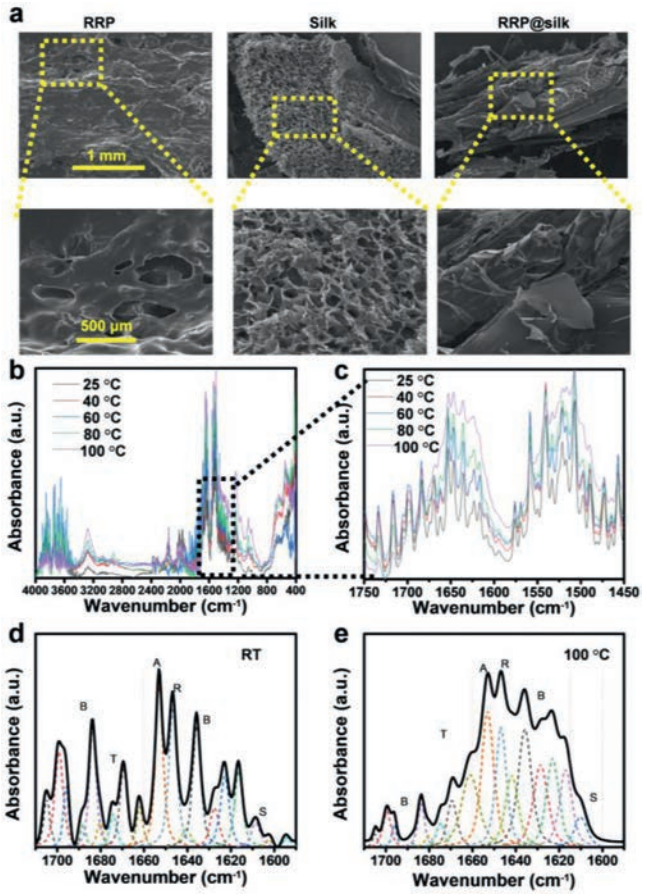

Fig. 3. Characterization of RRP@silk film. (a) Scanning electron microscope of RRP, silk and RRP@silk. (b) Fourier transform infrared spectroscopy of silk protein (4000–400 cm^{-1} normalized full spectrum). (c) Fourier transform infrared spectroscopy of silk (1750–1450 cm^{-1}, normalized partial spectrum). (d) Fourier deconvolution linear fitting of silk protein at room temperature (lateral chain (S), β-sheet (B), β-turn (T), α-helix (A), random coil (R), (1700–1600 cm^{-1})). (e) Fourier deconvolution linear fitting of silk protein at 100 °C for 10 h. (lateral chain (S), β-sheet (B), β-turn (T), α-helix (A), random coil (R), (1700–1600 cm^{-1})).

the RRP@silk film, the marriage of RRP solution (100 mg/mL) and aqueous silk solution (50 mg/mL) with different proportion (1:1, 1:5, 1:10, 1:20) was prepared. As shown in Fig. 2b, with the increment of RRP solution content in the RRP@silk film, the temperature raised at a high speed. Noteworthily, the ΔT was dropped from 80 °C to 30 °C with the RRP proportion decreased from 1:1 to 1:20, while the silk solution as control group scarcely showed any temperature elevation during the experiment. Meanwhile, the absorption of pristine silk solution, RRP@silk solution (1:20) and RRP solution in the vis-NIR region were also investigated (Fig. 2c). The absorption value of RRP@silk solution (1:20) at 808 nm was much higher than pristine silk solution, but lower than RRP solution, indicating the successful confusion of RRP solution and pristine silk solution. Thus, the proportion of RRP solution and pristine silk solution was chosen for 1:20 for future application which suited perfectly in following studies.

To deeply evaluate the morphology difference between silk and RRP@silk film, the scanning electron microscope was employed to observe it. The morphology of silk was loose and porous, and the pores and sheet number were much more than the RRP (Fig. 3a). The pores and sheet number of RRP@silk film were between the silk and RRP, suggesting that RRP@silk film was successful synthesis and combining both advantage of silk and RRP. It had reported that the β-sheet proteins in silk had critical functions in biology, such as recombining the enzymatic processing of biochemical reaction in carbohydrates and transporting the small and hydrophobic molecules in our cells and blood [45]. In our study, the Fourier transform infrared spectroscopy was used to study the change of silk protein in different temperatures. The change of lateral chain (S), β-sheet (B), β-turn (T), α-helix (A), and random coil (R) were showed in different temperature including 25 °C, 40 °C, 60 °C, 80 °C, 100 °C (Figs. 3b and c) [46]. With the increasement of temperature, the absorbance of β-sheet had enhanced, suggesting the protein change of secondary structure [47]. The biggest change of silk protein was under the temperature of 100 °C (Figs. 3d and e). The absorbance of β-sheet and random coil were significantly increased. The crystallinity of silk protein was increased from 29.85% to 40.89%. All above-mentioned results showed that temperature increasement could enhanced the absorbance of β-sheet, suggesting the increasement of β-sheet structure. Meanwhile, considering of the *in vivo* treatment, we had decided the 60 °C for further use [27].

To further assess the photothermal and healing capacity of RRP@silk film, *in vivo* skin wound healing experiment was carried out by using BALB/c mice model. Twenty BALB/c mice were randomly assigned to four groups with only five in each group, which were named as control, NIR, RRP@silk and RRP@silk + NIR groups respectively. When skin wound was successfully fitted with RRP@silk film, the infrared thermal camera was employed to monitor the temperature change during laser irradiation while the output power was set as 1 W/cm^2. As showed in Fig. 4a, the temperature in the wound region raised smoothly from 35.3 °C to 62.7 °C within 3 min in RRP@silk + NIR group, which was high enough to make the silk protein to interact with the wound area [48] and establish robust silk fibroin micro stents immediately that could promote multifarious cell growth and migration [49]. Furthermore, the laser irradiation did not do harm to the nearby skin because of the precise irradiation [50] and rapid cooling of the wound area. After the treatments, the wound pictures were taken every two days for

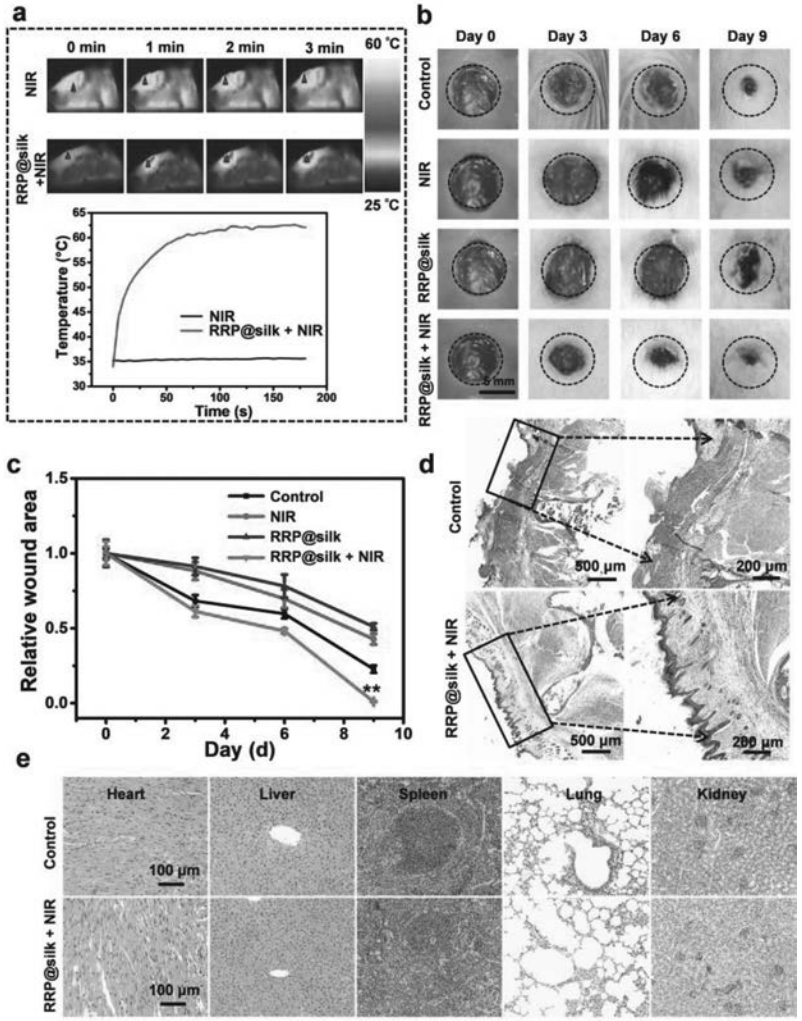

Fig. 4. *In vivo* skin wound healing evaluation of RRP@silk film. (a) Infrared images and temperature elevation of skin wound healing mice under laser irradiation (808 nm, 1 W/cm^2) without or with the treatment of RRP@silk (RRP:silk = 1:20). (b) Photograph and (c) relative quantification of wound area of the control, NIR, RRP@silk and RRP@silk + NIR group on day 0, day 3, day 6 and day 9. ** $P < 0.01$. (d) Representative H&E images of skin wound obtained from the mice on day 9 after the mice sacrifice. (e) Representative H&E images of the major organs (including heart, liver, spleen, lung, and kidney) of the control group and the RRP@silk + NIR group on day 9 after the mice sacrifice.

recording the effects. As showed in Figs. 4b and c, the skin wounds of RRP@silk + NIR group were healing faster and better than other three groups. The surface of whole skin wound was almost intact and seemed like original shape, suggesting that RRP@silk film indeed contributed to skin wound healing with the assistance of NIR laser. At day 9, the mice were all sacrificed and the wound tissues were extracted. H&E staining of the correlative skin wound tissues were performed to show that the skin had the whole epidermis and dermis in the RRP@silk + NIR group (Fig. 4d). It is obvious to see that the sebaceous glands, sweat gland and hair follicles grew toward the middle of the wound, indicating that the skin wound had healed completely and gradually returned to normal tissue. On the contrary, the epidermis, dermis tissue and other skin appendages of other three groups were still fractured or nonexistent. These results suggested that the RRP@silk film possessed the excellent photothermal and healing capacity which could be applied in clinical research.

Inspired by the outstanding performance for skin wound healing, we are curious about its effect for skin incision healing. Therefore, the RRP@silk film for skin incision healing was performed, and the processes were almost the same as before, except that the skin wound healing model was transferred to skin incision healing model [51]. Ten BALB/c mice were randomly assigned to two groups including control and RRP@silk + NIR groups. After the treatment, the skin incision of RRP@silk + NIR group were entire coalescence and healed better and more complete than control group (Fig. S1a in Supporting information). The BALB/c mice were anesthetized by CO_2 inhalation and cervical dislocation at day 5. The corresponding incision tissues slices by H&E staining were shown in Fig. S1b (Supporting information), which showed that there still existed an apparent incision in the control group. Meanwhile, the incision was almost healed in the RRP@silk + NIR group, suggesting the excellent effect of the RRP@silk film in skin incision healing model.

Toxicity is another big bottleneck for sealant agent for future clinical application. To evaluate the toxicity of RRP@silk film *in vivo*, major organs (heart, liver, spleen, lung, and kidney) of mice were extracted from control group and RRP@silk + NIR group after the treatments in day 9 [38]. According to the H&E staining results, there was no significant change in major organs between two groups (Fig. 4e). It demonstrated that there was no obvious toxicity of the RRP@silk film. These findings had laid the foundation and expanded another field for the future skin repair research or other clinical application.

In summary, RRP possessed excellent photothermal conversion of 63.7% and high photothermal stability. Therefore, the temperature of RRP@silk film could raise to 60.0 °C within 3 min. At that temperature, abundant of silk protein changed the form of α-helix to β-sheet or tertiary structure, indicating the new-born cell could migrate more convenient with the contribution of β-sheet silk protein, so that skin incision and wound could heal faster. Importantly, RRP@silk film showed negligible toxicity *in vivo*. Compared with other skin incision or wound healing agents, here, RRP and silk were married and developed as a novel therapy agent in a facile and low-cost way, where RRP worked as a suitable photothermal material and silk works as robust/biomimetic protein material. We hoped that this new methodology can provide insights into the applications of traditional RRP and silk in biomedical fields.

Declaration of competing interest

The authors declare no conflict of interest.

Acknowledgments

This study was supported by the National Natural Science Foundation of China (Nos. 81972488 and 81973013), the Eighth Affiliated Hospital of Sun Yat-sen University Outstanding Youth Reserve Talent Science Fund (No. FBJQ2019002), the Guangdong Key R&D Program (No. 2019B020210002), the Guangdong Natural Science Foundation (No. C1051164), China Postdoctoral Science Foundation (Nos. 2019TQ0242, 2019M660061XB).

Supplementary materials

Supplementary material associated with this article can be found, in the online version, at doi:10.1016/j.cclet.2021.09.018.

References

[1] H.D. Zomer, A.G. Trentin, J. Dermatol. Sci. 90 (2017) 3–12.
[2] J.A. Sanford, R.L. Gallo, Semin. Immunol. 25 (2013) 370–377.
[3] J. Khavkin, D.A. Ellis, Facial. Plast. Surg. CL. 19 (2011) 229–234.
[4] A.V. Nguyen, A.M. Soulika, Int. J. Mol. Sci. 20 (2019) 1811.
[5] S. Papastefan, C. Buonpane, G. Ares, et al., J. Surg. Res. 242 (2019) 70–77.
[6] K. Kiya, T. Kubo, Neurochem. Int. 125 (2019) 144–150.
[7] C. Zhang, H. Liang, D. Liang, et al., Angew. Chem. Int. Ed. 60 (2021) 4289–4299.
[8] E.Y. Jeon, B.H. Hwang, Y.J. Yang, et al., Biomaterials 67 (2015) 11–19.
[9] X. Wang, H. Liang, J. Jiang, et al., Green Chem. 22 (2020) 5722–5729.
[10] L. Liu, J. Lu, Y. Zhang, et al., Green Chem. 21 (2019) 526–537.
[11] D.N. Rockwood, R.C. Preda, T. Yucel, et al., Nat. Protoc. 6 (2011) 1612–1631.
[12] J.R. Mauney, T. Nguyen, K. Gillen, et al., Biomaterials 28 (2007) 5280–5290.
[13] H.W. Ju, O.J. Lee, J.M. Lee, et al., Int. J. Biol. Macromol. 85 (2016) 29–39.
[14] A. Sugihara, K. Sugiura, H. Morita, et al., P. Soc. Exp. Bio. Med. 225 (2010) 58–64.
[15] M. Pollini, F. Paladini, Materials (Basel) 13 (2020) 3361.
[16] W. Sun, D.A. Gregory, M.A. Tomeh, X. Zhao, Int. J. Mol. Sci. 22 (2021) 1499.
[17] L. Meinel, S. Hofmann, V. Karageorgiou, et al., Biomaterials 26 (2005) 147–155.
[18] A.M. Chiarini, P. Petrini, S. Bozzini, I.P. Dal Pra, U. Armato, Biomaterials 24 (2003) 789–799.
[19] M. Woltje, M. Bobel, M. Bienert, et al., J. Biomed. Mater. Res. A 106 (2018) 2643–2652.
[20] M. Gizaw, J. Thompson, A. Faglie, et al., Bioengineering 5 (2018) 9.
[21] J.J. Khadem, M. Martino, F. Anatelli, M.R. Dana, M.R. Hamblin, Laser Surg. Med. 35 (2004) 304–311.
[22] Y. Wang, D. Zhang, K. Xiong, R. Shang, X.D. Jiang, Chin. Chem. Lett. 33 (2022) 115–122.
[23] L. Sun, Y. Shi, M. Tang, et al., Nanoscale 11 (2019) 14237–14241.
[24] H. Wu, C. You, F. Chen, et al., Mater. Sci. Eng. C 103 (2019) 109738.
[25] D. Jia, X. Ma, Y. Lu, et al., Chin. Chem. Lett. 32 (2021) 162–167.
[26] N. Jiang, Z. Zhou, W. Xiong, et al., Chin. Chem. Lett. 32 (2021) 3948–3953.
[27] R. Urie, C. Guo, D. Ghosh, et al., Adv. Funct. Mater. 28 (2018) 1802874.
[28] X. Meng, M. He, R. Guo, et al., Molecules 22 (2017) 1193.
[29] U.J. Youn, B. Gu, K. Kim, C. Ha, I.C. Jung, J. Pharmacopunct. 21 (2018) 112–119.
[30] C. Liu, R. Ma, L. Wang, et al., J. Ethnopharmacol. 198 (2017) 351–362.
[31] C. Wu, J. Shan, J. Feng, et al., Fish. Shellfish Immun. 89 (2019) 641–646.
[32] Y. Wang, M. Kwak, P.C.W. Lee, J. Jin, Inter. J. Bio. Macromol. 116 (2018) 232–238.
[33] J.Y. Jhun, H.S. Na, J.W. Shin, et al., J. Med. Food 21 (2018) 745–754.
[34] Z. Miao, K. Li, P. Liu, et al., Adv. Healthc. Mater. 7 (2018) 1701202.
[35] I.J. Chetty, M.K. Martel, D.A. Jaffray, et al., Inter. J. Radiat. Oncol. 93 (2015) 485–492.
[36] W. Chen, J. Ouyang, H. Liu, et al., Adv. Mater. 29 (2017) 1603864.
[37] M. Hou, C. Yan, Z. Chen, et al., Acta Biomater. 74 (2018) 334–343.
[38] B. Guo, Z. Sheng, D. Hu, et al., Adv. Mater. 30 (2018) 1802591.
[39] M. Xu, K. Zhang, Y. Liu, et al., Colloids Surf. B: Biointerfaces 184 (2019) 110551.
[40] J. Xu, B. Xia, X. Niu, et al., Dyes Pigments 170 (2019) 107664.
[41] M. Lee, C. Lee, H.S. Jung, et al., ACS Nano 10 (2016) 822–831.
[42] R. Deng, M. Zou, D. Zheng, et al., ACS Nano 13 (2019) 8618–8629.
[43] L. Huang, M. Liu, H. Huang, et al., Biomacromolecules 19 (2018) 1858–1868.
[44] Y. Gao, S. Wu, Y. Sun, et al., Dry. Technol. 37 (2019) 1427–1440.
[45] E. Marcos, T.M. Chidyausiku, A.C. McShan, et al., Nat. Struct. Mol. Biol. 25 (2018) 1028–1034.
[46] T. Kawasaki, T. Yaji, T. Ohta, K. Tsukiyama, K. Nakamura, Cell. Mol. Neurobiol. 38 (2018) 1039–1049.
[47] M. Iglesiasbexiga, M. Szczepaniak, C.S. de Medina, et al., J. Phys. Chem. B 122 (2018) 11058–11071.
[48] P. Matteini, F. Sbrana, B. Tiribilli, R. Pini, Laser Med. Sci. 24 (2009) 667–671.
[49] M. Mushaben, R. Urie, T. Flake, et al., Laser Surg. Med. 50 (2018) 143–152.
[50] S. Wang, X. Liu, B. Li, et al., Adv. Funct. Mater. 29 (2019) 1904093.
[51] H. Xue, L. Hu, Y. Xiong, et al., Carbohyd. Polym. 226 (2019) 115.